# Supersonic flow over a Double-Wedge Airfoil

**Mridu Sai Charan A S**

# Contents

# List of Figures

# List of Tables

# Chapter 1

# Introduction

Supersonic speeds are associated with shocks and expansion fans. Shocks are classified as normal shocks and oblique shocks. Shocks are basically pressure waves which distinguish a region of higher and lower pressures. Normal shocks are stronger than oblique shocks and can be observed in internal flows such as a nozzle or a pipe. Oblique shocks are usually observed when obstacles or inclined walls are present. Since flow around an airfoil is an external flow, oblique shocks are formed exclusively. Since shockwaves are primarily pressure waves, they extend a lot of unnecessary considerations for aircraft wing designs. One such example is vibrations due to which, fastening with rivets or screws need to be designed and special considerations need to be made.

Supersonic airfoils can be classified into double wedge and convex airfoils. Generally, double wedge airfoils produce more lift at supersonic conditions but are less efficient in comparison to convex airfoils at subsonic speeds. In addition, if double wedge airfoils are used, aerothermodynamics need to be considered as the temperatures at the airfoil tips may reach the materials melting points[1][3][5].

Tellez et al.,[9] present a numerical simulation and experimental study on oblique shockwave over symmetrical double-wedge airfoil. The commercial CFD package Ansys Fluent was used to perform the numerical investigation. This study aims to perform similar calculations on a double-wedge airfoil using OpenFoam which is an open source CFD solution package. However, the current study is not just restricted to the work by Tellez, it is infact extended to a number of angles of attack in order to plot a L/D vs AoA.

Most of the discussions on Gas Dynamics in the subsequent sections are referenced from Dr. E. Rathakrishnan's text book on Gas Dynamics [7] as well as Dr. John D Anderson's text book [2]

# Chapter 2

# Gas Dynamics - An overview

## 2.1 Introduction

Gas dynamics is the study of flow in which density and temperature changes are significant($> 5\%$). The gas dynamics flow regimes consist of both subsonic and supersonic flows. When the flow is supersonic, the changes in flow properties or flow direction is caused by pressure waves. These waves can be compression (shock) waves, expansion waves, and Mach waves.

In engineering applications, such as the design of airplanes, missiles, and launch vehicles, the flow Mach numbers associated are more than 0.5. Hence both temperature and density changes associated with the flow become significant.

In gas dynamics, a change of state in flow properties is achieved by three means:

- with area change, treating the fluid as inviscid and passage to be frictionless - *Isentropic Flow*
- with friction, treating the heat transfer between the surroundings and the system to be negligible - *Fanno or Frictional Flow*
- with heat transfer, assuming the fluid to be inviscid. - *Rayleigh Flow*

Although it is impossible in practice to have a flow process which is purely isentropic or Fanno type or Rayleigh type, these assumptions are justified, since the results obtained with these treatments prove to be accurate enough for most practical problems in gas dynamics.

Compressibility is the phenomenon by virtue of which the flow changes its density with changes in speed. The change in volume is the characteristic feature of a compressible medium under static conditions.Under dynamic conditions, that is when the medium is moving, the characteristic feature for incompressible and compressible flow situations are:

- the volume flow rate, $\dot{Q} = AV = constant$; at any cross-section of a streamtube for incompressible flow
- the mass flow rate, $\dot{m} = \rho AV = constant$; at any cross-section of a streamtube for compressible flow.

## 2.2 Shocks and their Classifications

Shock is a compression front across which the flow properties jump. Shock may also be described as a front in a supersonic flow field, and the flow processing across the front results in an abrupt change in fluid properties. In other words, shock is a thin region where large gradients in temperature, pressure, and velocity occur and where the transport phenomena of momentum and energy are important. The thickness of the shocks is comparable to the mean free path of the gas molecules in the flow field.

Shock waves can be classified into:

- **Normal Shocks** which are at $90^0$ (perpendicular) to the flow direction
- **Oblique Shocks** which are at angle to the direction of flow
- **Bow Shocks** Occurs upstream of the front (bow) of a blunt object when the upstream flow velocity exceeds Mach 1.

**Shock front:** The boundary across which the properties like pressure, density and temperature undergo an abrupt change due to the presence of a shock wave is called a shock wave.

### 2.2.1 Normal Shock Equations

A shock can be moving or stationary for example, an obstacle placed in a flow region forms a stationary shock. Across a normal shock, the speed of sound also experiences a change. Therefore, a characteristic speed of sound, $a^*$ is defined with the following equation (relating $a_1$ and $a_2$).

$$\frac{V_1^2}{2} + \frac{a_1^2}{\gamma - 1} = \frac{V_2^2}{2} + \frac{a_2^2}{\gamma - 1} = \frac{1}{2}\frac{\gamma + 1}{\gamma - 1}a^{*2} \tag{2.1}$$

and, $a^*$ is also defined using the Prandtl relation as:

$$a^{*2} = V_1 V_2 \tag{2.2}$$

Mach Number relationship before and after the shock can be obtained using the relation:

$$M_2^2 = \frac{1 + \frac{\gamma-1}{2}M_1^2}{\gamma M_1^2 - \frac{\gamma-1}{2}} \tag{2.3}$$

The rise in pressure, density, and temperature downstream a normal shock can be calculated as follows:

$$\frac{p_2}{p_1} = 1 + \frac{2\gamma}{\gamma + 1}(M_1^2 - 1) \tag{2.4}$$

$$\frac{\rho_2}{\rho_1} = \frac{V_1}{V_2} = \frac{(\gamma + 1)M_1^2}{(\gamma - 1)M_1^2 + 2} \tag{2.5}$$

$$\frac{T_2}{T_1} = \frac{p_2}{p_1}\frac{\rho_1}{\rho_2} \tag{2.6}$$

The solutions to these equations at a particular upstream value of M can be referenced from a table called normal shock table as an alternative to solving the above equations.

### 2.2.2 Oblique Shock Equations

An oblique shock wave is a shock that, is inclined with respect to the incident upstream flow direction. It occurs when a supersonic flow encounters a corner that turns the flow into itself. The most common example used produce an oblique shock is to place a wedge in a supersonic flow. While the flow direction is unchanged across a normal shock, for an oblique shock, it changes direction.

$$\tan\theta = 2\cot\beta\frac{M_1^2\sin^2\beta - 1}{M_1^2(\gamma+\cos 2\beta)+2} \tag{2.7}$$

Where, the Equation 2.7 is called the $\theta - \beta - M$ relation, $\theta$ is the flow deflection angle, $\beta$ is the shock angle and $M_1$ is the upstream Mach Number. The rise in pressure, density, and temperature after an oblique shock can be calculated as follows:

$$\frac{p_2}{p_1} = 1 + \frac{2\gamma}{\gamma+1}(M_1^2\sin^2\beta - 1) \tag{2.8}$$

$$\frac{\rho_2}{\rho_1} = \frac{(\gamma+1)M_1^2\sin^2\beta}{(\gamma-1)M_1^2\sin^2\beta+2} \tag{2.9}$$

$$\frac{T_2}{T_1} = \frac{p_2}{p_1}\frac{\rho_1}{\rho_2} \tag{2.10}$$

Further, the downstream Mach Number is solved for using:

$$M_2 = \frac{1}{\sin(\beta-\theta)}\sqrt{\frac{1+\frac{\gamma-1}{2}M_1^2\sin^2\beta}{\gamma M_1^2\sin^2\beta - \frac{\gamma-1}{2}}} \tag{2.11}$$

The solutions to these equations at a particular M and $\beta$ can be referenced from a table called oblique shock table instead of solving the above equations.

## 2.3 Expansion Fans

When a supersonic flow is made to turn away from its initial direction, it experiences a loss in pressure after the turn. This reduction in pressure occurs when the flow is said to pass through an expansion fan at the turn. When a flow goes through an expansion process, the Mach lines diverge as shown in Figure 2.1, and consequently, there is a tendency to decrease the pressure, density, and temperature of the flow passing through them. This phenomenon is isentropic throughout.

### 2.3.1 Prandtl-Meyer Expansion

A supersonic expansion fan, technically known as Prandtl–Meyer expansion fan, a two-dimensional simple wave, is a centered expansion process that occurs when a supersonic flow turns around a convex corner. The fan consists of an infinite number of Mach waves, diverging from a sharp corner. When a flow turns around a smooth and circular corner, these waves can be extended backwards to meet at a point.

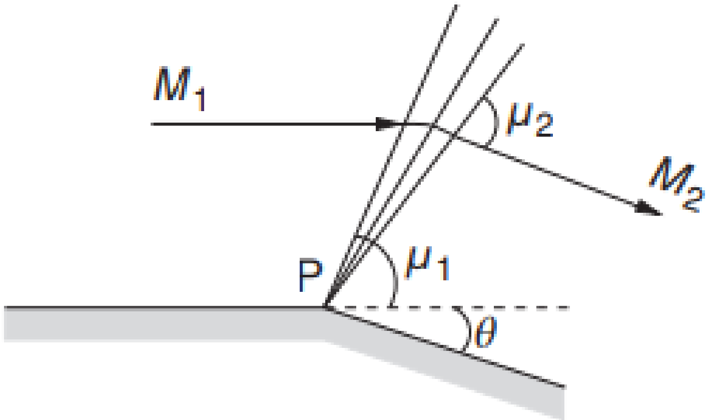


Figure 2.1: Expansion Fan at a Corner

### 2.3.2 Prandtl-Meyer Function

The calculation of the expansion fan involves the use of the Prandtl-Meyer function. This function is derived from conservation of mass, momentum, and energy for very small (differential) deflections. The Prandtl-Meyer function is denoted by the Greek letter $\nu$ on the slide and is a function of the Mach number M and the ratio of specific heats of the gas.

$$\nu = \sqrt{\frac{\gamma+1}{\gamma-1}} \arctan \sqrt{\frac{\gamma+1}{\gamma-1}(M_1^2-1)} - \arctan \sqrt{(M_1^2-1)} \qquad (2.12)$$

The Mach number of a supersonic flow increases through an expansion fan. The amount of the increase depends on the incoming Mach number and the angle of the expansion. The physical interpretation of the Prandtl-Meyer function is that it is the angle through which a sonic (M=1) flow needs to be expanded to obtain a given Mach number. The value of the Prandtl-Meyer function is therefore called the Prandtl-Meyer angle.

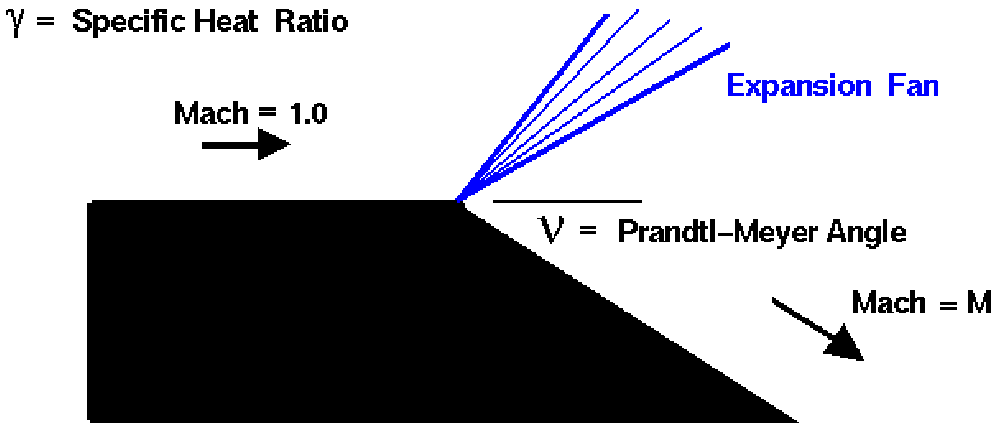


Figure 2.2: Prandtl Meyer Angle

## 2.4 Flow over a wedge

Supersonic flow over a wedge involves two of the three phenomena discussed in the previous sections. Wherever the flow is relatively turned away from its initial direction, an expansion fan is formed, and wherever the flow turns into itself, an oblique shock is formed.

In Figure 2.3, region 1 can be considered as the free stream region where the flow is moving from right to left without any deflections and at a constant mach number. Due to the presence of the airfoil, the flow is split and one stream flows above the airfoil and one below. Considering the flow above airfoil, the flow further changes its direction before a final deflection to reach state 4 where it will again reach free stream conditions. Similar behavior can be observed in below the airfoil as well.

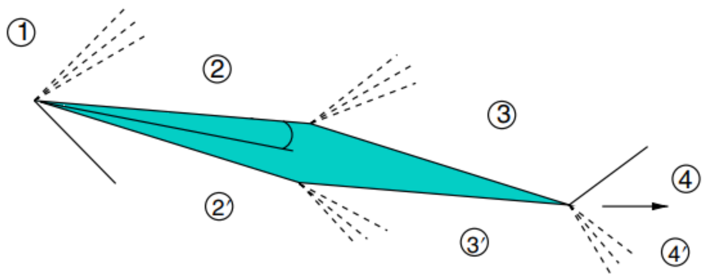


Figure 2.3: Supersonic Flow over an Inclined Wedge

In terms of regions, the flow can be explained as follows.

### Above the Airfoil

- **From 1 - 2** Expansion fan is formed as the flow turns away from its direction at 1.
- **From 2 - 3** Once again, an expansion fan is formed as the flow turns away from its direction at 2.
- **From 3 - 4** In this transition, the flow tries to reverse the deflections undergone by the flow at **1 - 2** and **2 - 3** and therefore an oblique shock is formed.

### Above the Airfoil

- **From 1 - 2′** Oblique shock is formed as the flow turns into itself.
- **From 2′ - 3′** Due to geometry, the flow turns away from its direction at 2′ the magnitude of the deflection and the pressure difference it causes depends on the geometry of the wedge.
- **From 3′ - 4′** In this transition, the flow tries to correct any remaining deflections such that initial (1) freestream conditions are reached.

It is interesting to note here that while 4 and 4′ are expected to be at the same freestream conditions, they are not designated by one number/alphabet. This is due to the fact that a slipstream may or may not exist in the wake of the airfoil due to flow symmetry.

# Chapter 3

# Theory

## 3.1 Concept

Two dimensional compressible flows of a calorically perfect gas are modeled with governing equations that couple the conservations of mass, momentum in x-y directions, and energy. Therefore, they need be solved simultaneously. CFD techniques are developed to solve these equations numerically. In order to find the delicate balance between solution accuracy as well as computational costs, quite a few studies were conducted, and new solution schemes were developed. CFD was not a viable option for many fluid flow problems due to limited computational resources. But, in today's world, CFD studies which are not limited by complex tasks such as catching shock location accurately, shock boundary layer interaction etc can be run on any personal computer.

For the problem statement at hand, an airfoil subjected to a supersonic speed is considered. The flow regime around the airfoil is mainly governed by three equations, namely, the mass continuity equation, the momentum conservation as well as energy conservation equations. These equations can be written as:

$$\frac{\partial \rho}{\partial t} + \nabla \cdot (\rho u) = 0 \tag{3.1}$$

$$\frac{\partial}{\partial t} \iiint_{\Omega} \rho u \, d\Omega = \oiint_{S} (\rho u \cdot dS) u - \oiint_{S} p dS + \iiint_{\Omega} \rho F_{Body} d\Omega + F_{surf} \tag{3.2}$$

$$\rho \frac{Dh}{Dt} = \frac{Dp}{Dt} + \nabla \cdot (k \nabla T) + \psi \tag{3.3}$$

Where, equation 3.1 governs the rate of change of fluid mass in a control volume $\Omega$, equation 3.2 is the equation that governs unsteady, viscous supersonic flows (The momentum conservation equation) and equation 3.3 governs the law of conservation of energy. The $\psi$ refers to the viscous dissipation function.

## 3.2 Geometry and Meshing

To study the flow around an airfoil, various types of computational domains are used, rectangular, C - inlet, O domains, etc to name a few. For the purpose of the present study a rectangular domain as presented in the Abstract Section, that is, ?? was used since since the boundary conditions that are applied are simplistic.

The mesh used in this study is a structured mesh. The size of the element size in the mesh along with justification for the same is provided in the Mesh Independence Section. A schematic of the mesh used for the 0 AoA case is given in the Figure 3.1.

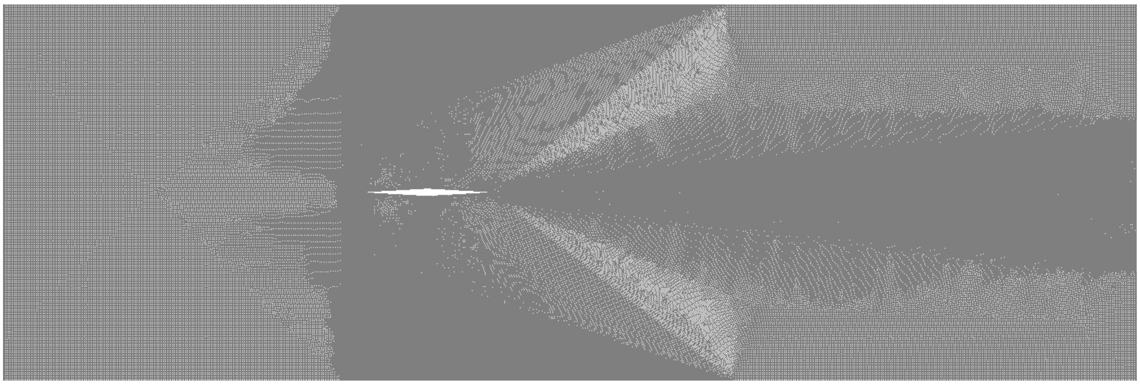

Figure 3.1: Mesh used in the Study

## 3.3 Turbulence Modeling

To ensure a practical approach, the standard k-$\epsilon$ turbulence model as proposed by Launder and Spalding [6] is used which is based on minimizing unknown variables present in the exact k-$\epsilon$ model. The equations describing the two transport variables: the turbulent kinetic energy, k and the rate of dissipation of the turbulent kinetic energy, $\epsilon$ are presented in 3.4 and 3.5

$$\frac{\partial \rho k}{\partial t} + \frac{\partial \rho k u_i}{\partial x_i} = \frac{\partial [\frac{\mu_t}{\sigma_k}\frac{\partial k}{\partial x_j}]}{\partial x_j} + 2\mu_t E_{ij} E_{ij} - \rho\epsilon \tag{3.4}$$

$$\frac{\partial \rho \epsilon}{\partial t} + \frac{\partial \rho \epsilon u_i}{\partial x_i} = \frac{\partial [\frac{\mu_t}{\sigma_k}\frac{\partial \epsilon}{\partial x_j}]}{\partial x_j} + C_{1\epsilon}\frac{\epsilon}{k} 2\mu_t E_{ij} E_{ij} - C_{2\epsilon}\rho\frac{\epsilon^2}{k} \tag{3.5}$$

Where, $u_i$ is the velocity component in $i^{th}$ direction, $E_{ij}$ is the component of rate of deformation, $\mu_t = \rho_\mu \frac{k^2}{\epsilon}$, is the eddy viscosity.

Further, from the work of Versteege[4], the values for a few specific constants like $C_\mu$, $\sigma_k$, $\sigma_\epsilon$, $C_{1\epsilon}$, $C_2\epsilon$ have been set.

## 3.4 Solver Setup and Boundary Conditions

The Open Source Field Operation and Manipulation (OpenFOAM)[10] is an open source CFD package that is coded in C++. It has a variety of finite volume solvers for both structured and unstructured girds. The code includes the solvers for several specific flow conditions, such as, steady, unsteady, laminar, turbulent flows, etc. In the current study, the sonicFoam solver which is coded specifically for compressible flows is used.

The sonicFoam solver is a transient transonic/supersonic, laminar or turbulent solver used for simulating a compressible flow. This solver uses the PIMPLE algorithm which is a combination of PISO (Pressure Implicit with Splitting of Operator) and SIMPLE (Semi-Implicit Method for Pressure-Linked Equations) algorithms. PISO and SIMPLE are iterative solvers. While, PISO and PIMPLE can be used for transient cases, SIMPLE can only be used for steady-state problems. Better solver stability is obtained when PIMPLE is used (Considering transient cases) when large time steps where the maximum Courant number may consistently be above 1 is encountered or when the solution is inherently unstable.

The free stream conditions of the flow before and after the airfoil are given in Table 3.1

| **Parameter** | **Value** |
|---|---|
| Mach Number | 2 |
| Temperature | 300K |
| X - Velocity | 650 m/s |
| Static Pressure | 1 atm |

Table 3.1: Free Stream Values

The boundary conditions used in this study are given as a table in 3.2

| **Variable** | **Inlet** | **Outlet** | **Top/Bottom Walls** | **Foil Wall** |
|---|---|---|---|---|
| Pressure | fixedValue | waveTransmissive (non reflective) | zeroGradient | zeroGradient |
| Velocity | fixedValue | inletOutlet | supersonicFreestream | noSlip |
| Temp | fixedValue | inletOutlet | inletOutlet | zeroGradient |
| $\alpha_T$ | calculated | calculated | calculated | alphatWallFunction |
| $\epsilon$ | fixedValue | inletOutlet | inletOutlet | epsilonWallFunction |
| Turb. KE | fixedValue | inletOutlet | inletOutlet | kqRWallFunction |
| $\nu$ | calculated | calculated | calculated | nutkWallFunction |

Table 3.2: Boundary Conditions

Where, for all the turbulence related terms, their respective wall functions are used at the foil wall. The top and bottom walls are named as walls for convenience. They in actuality, possess a far field boundary condition. Figure 3.2 shows the boundary conditions in the schematic.

## 3.5 Mesh Independence

Mesh independent solution is a CFD solution that doesn't rely on the type of mesh or the size of mesh that is being used. That is, it removes the subjectivity of the solution and makes it more general. In the current study, the mesh size is varied and the minimum size at which a general solution is obtained is used as a reference or baseline upon which mesh independence can be proved.

Usually, a mesh/grid independence test is done with a non-uniform coarser mesh, wherein the size of element is varied and its influence of the final solution after

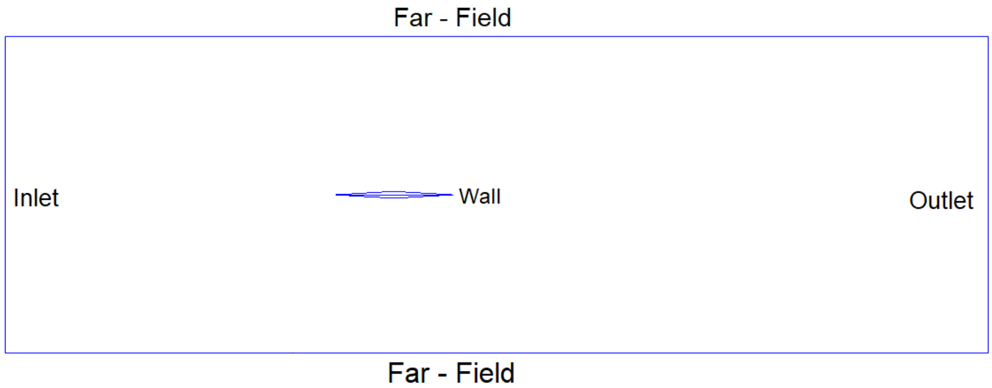


Figure 3.2: Boundary Conditions Used

convergence is studied. Mesh size is progressively reduced from a coarse size to a fine mesh size and the variation in flow parameters is checked. When the percentage difference between the two successive meshes is negligible, the coarser mesh can be used. Mesh independence forms an important part of CFD study to ensure that least computational resources are utilized.

Mesh Independence Study was performed for 3 cases which varied from one another on the basis of cell size. The three cases correspond to coarse, medium and fine meshes. The coarse mesh contains 150k cells, the medium mesh contains 300k cells and the fine mesh contains 450k cells.

Table 3.3 shows the variation in the chosen parameter, that is, lift between the 3 mesh sizes for 0 Angle of Attack case.

| **Mesh Size** | **Lift (N)** | **% Change** |
|---|---|---|
| Coarse | 4672 | - |
| Medium | 4498 | 3.86 |
| Fine | 4454 | 0.98 |

Table 3.3: Results for Lift at 0 AoA

Since, the error in lift between medium and fine mesh sizes is around $10^{-3}$ and therefore, the medium mesh has been chosen for the study.

# Chapter 4

# Results and Discussion

## 4.1 Courant Number

The Courant–Friedrichs–Lewy or CFL condition is a condition for the stability of unstable numerical methods that model convection or wave phenomena. As such, it plays an important role in CFD as it defines the length traversed on the grid during each timestep. This length should be less than one, that is, values for variables from a given element must move to the neighboring cells only.

It is often used as a rudimentary (not an absolute) measure of stability of the solver. It is also used as a reference in order to set the timestep. This condition is quantified using the Courant Number which is given as:

$$Co = u\frac{\Delta t}{\Delta x} \tag{4.1}$$

To ensure that this value is less that one, the following strategies can be utilized:

- Lowering the timestep
- Using a coarser mesh

Another alternative that can be used on OpenFOAM is to use the adjustable timestep feature and set the Courant number to a desired value. Thus, OpenFOAM lowers the timestep if required whenever the Courant number increases beyond the threshold that has been set.

In this study, the Courant number was restricted to a value of 0.3 however, there was no need to use the adjustable timestep feature as there were no convergence issues.

## 4.2 Mach Number

Though the free stream mach number might be a constant before the airfoil and after the airfoil, the mach number experiences signification changes on the airfoil walls both above and below. This is due to the presence of oblique shocks and expansion fans. Across an oblique shock, a decrease in mach number is observed whereas, across an expansion fan, an increase in mach number is observed. While at 0 angle of attack, this effect seems to be a very minute one, as the angle of attack increases, the difference in mach numbers also increase. For example, at angles of attack greater than 6, transonic mach numbers are found on the wall of the airfoil. This phenomenon is also observed for the increased mach number across expansion fans, that is, for 0 angle of attack, the increase in mach number after an expansion wave is a very small value above 2 but less than 2.1. However, at a high angle of attack, say 16 degrees, the mach number across an expansion fan is increased to 2.6 Mach.

Therefore, it can be concluded that as angle of attack is increased, the strength of the oblique shocks and expansion fans also increase. It is therefore important to study the contours of Mach number to intuitively understand the intricacies involved in such flows.

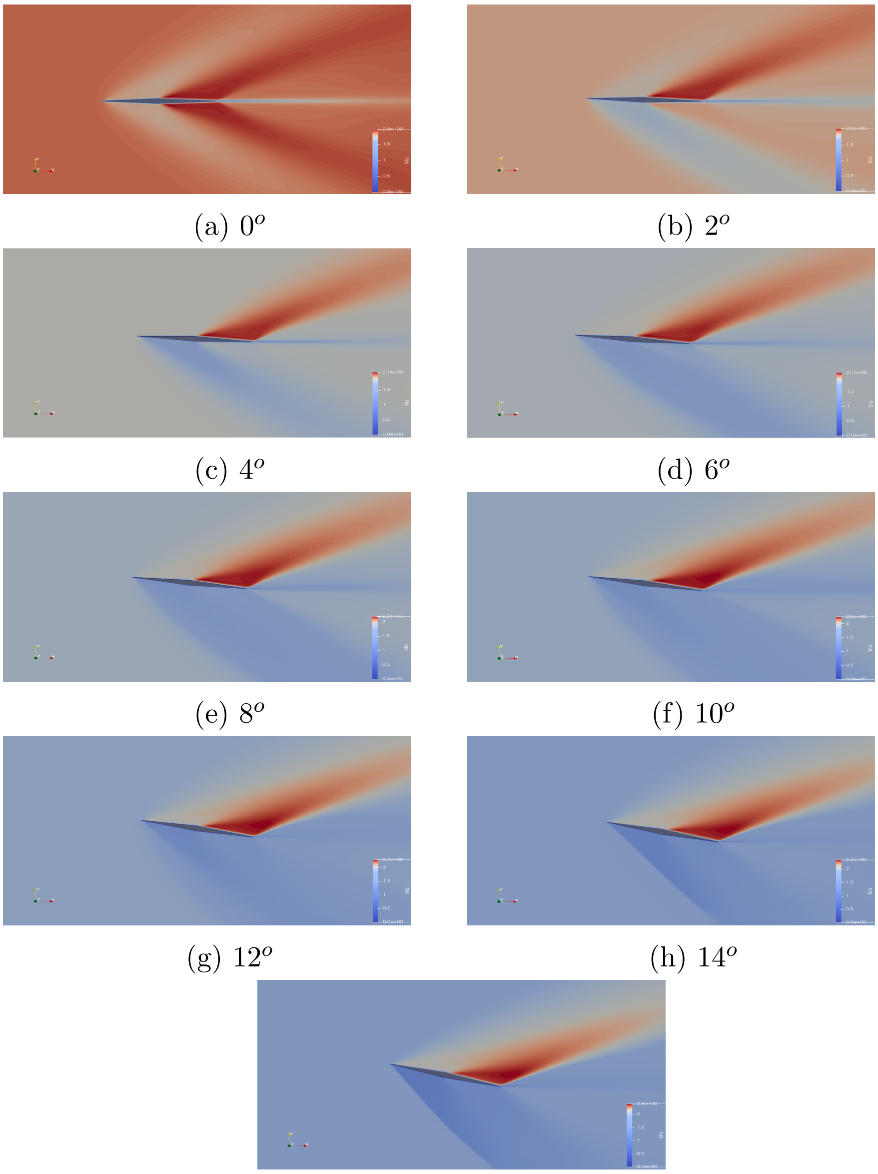

(a) $0^o$ (b) $2^o$

(c) $4^o$ (d) $6^o$

(e) $8^o$ (f) $10^o$

(g) $12^o$ (h) $14^o$

(i) $16^o$

Figure 4.1: Mach Number Contours at different Angles of Attacks

## 4.3 Pressure

Across a shock, an increase in pressure is observed and across an expansion fan, a decrease in pressure is observed. Further strengthening the conclusion drawn from the Ma contours is that as the angle of attack increases, the strengths of shocks and expansion fans increase. This leads to an increase in the rise of pressure post shock or a decrease in pressure post expansion fans.

This phenomenon can be clearly observed in the given contours. The increase and simultaneous decrease in pressure above and below the airfoil increase as the angle of attack increases and therefore, can be interpreted as the pressure difference at the bottom of the airfoil and the top of the airfoil increasing as a function of angle of attack. This fact can be used to explain the high lift that is obtained at high angles of attack.

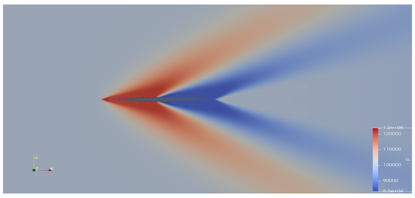

(a) $0^o$

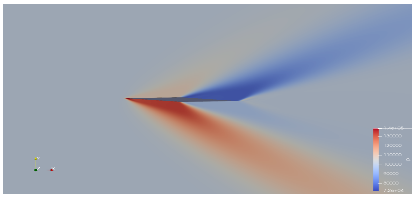

(b) $2^o$

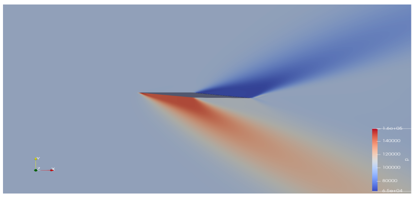

(c) $4^o$

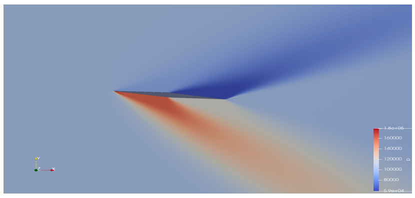

(d) $6^o$

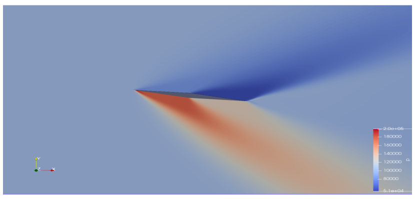

(e) $8^o$

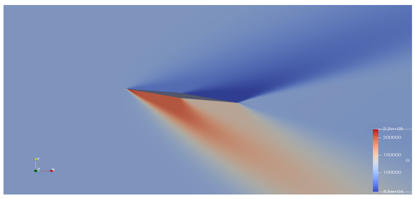

(f) $10^o$

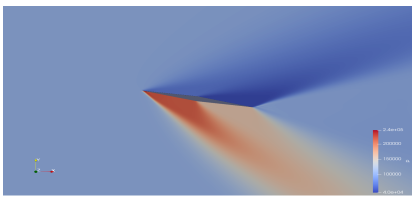

(g) $12^o$

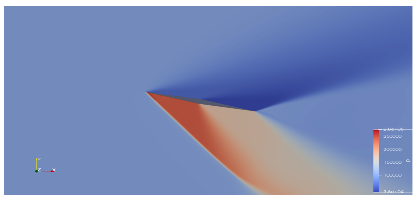

(h) $14^o$

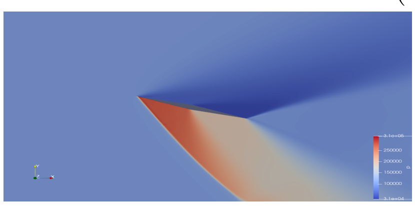

(i) $16^o$

Figure 4.2: Pressure Contours at different Angles of Attacks

## 4.4 Temperature

While temperature might not seem to be an important factor while discussing flow over a supersonic airfoil, it plays a very important role in the designing of wings or other structures that employ the supersonic airfoil. The materials that are used in manufacturing largely depend on the surface temperatures. As such, due to the presence of shocks and expansion fans, the temperature is not constant throughout. Post shocks, there is a visible increase in temperature and post expansion fans, there is a decrease in temperature. There are two factors that influence the increase or decrease in temperatures: free stream mach number, and angle of attack. As the free stream mach number or the angle of attack increase, the temperature differences increases. Therefore, for extreme cases of supersonic vehicles like atmospheric re-entry vehicles, there is a need to design shields for high temperatures at the tip of the airfoil and mechanisms to prevent icing towards the rear.

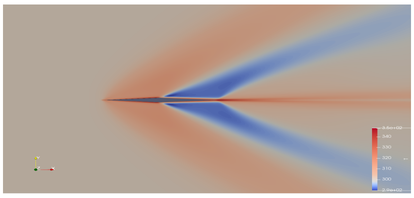

(a) $0^o$

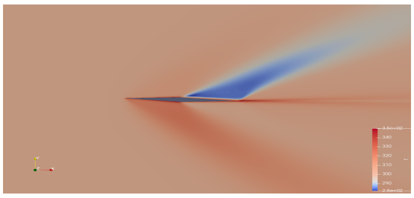

(b) $2^o$

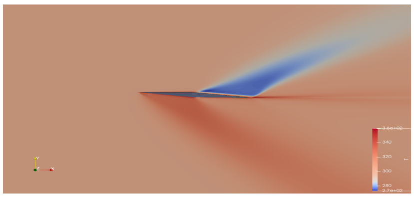

(c) $4^o$

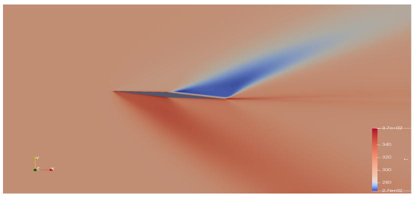

(d) $6^o$

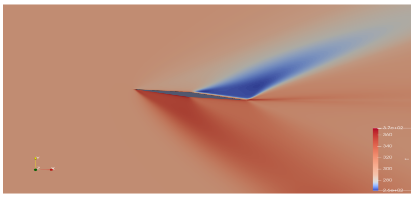

(e) $8^o$

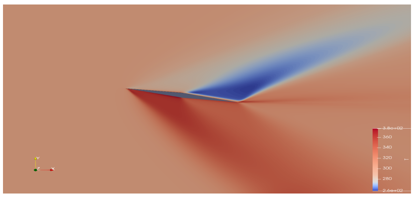

(f) $10^o$

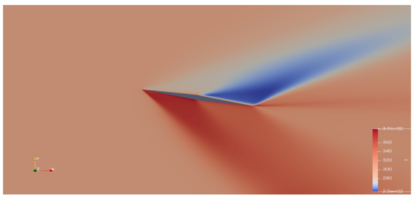

(g) $12^o$

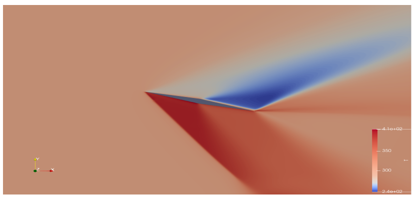

(h) $14^o$

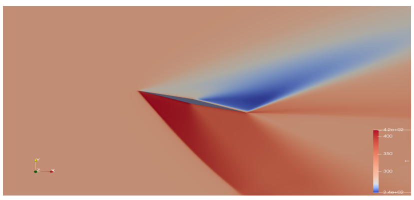

(i) $16^o$

Figure 4.3: Temperature Contours at different Angles of Attacks

## 4.5 Lift and Drag

The lift to drag ratio (or L/D ratio) is the ratio of lift generated to the aerodynamic drag it creates. Aircrafts are generally designed in order to maximise this quantity as a particular aircraft's lift is determined by its weight. A low L/D ratio results in lower fuel efficiency and consequently increased operating costs.

This ratio is generally calculated as a function of airspeed in the case of aircrafts. For airfoils, this ratio is calculated for a particular airspeed but at different angles of attack. Figure 4.4 shows a plot of L/D ratio to the angle of attack.

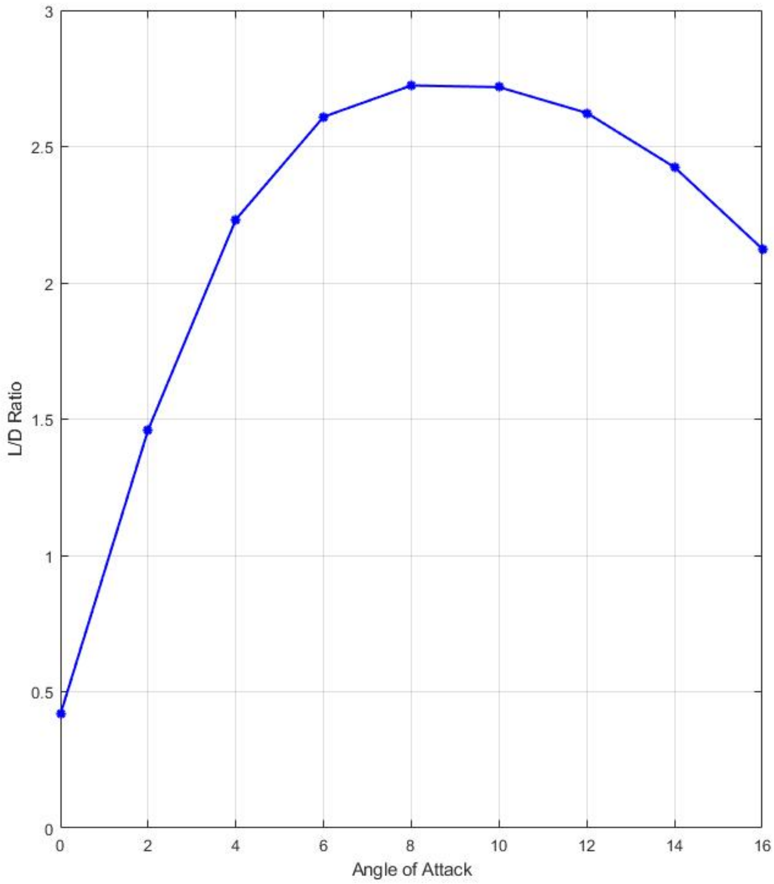


Figure 4.4: Plot of L/D Ratio and Angle of Attack

# Chapter 5

# Conclusion

## 5.1 Conclusion

A numerical study was conducted to investigate supersonic flow over a double wedge airfoil. The effect of increasing the angle of attack on Mach number, Pressure and Temperature was investigated. In addition, a plot of L/D ratio to the angle of attack was plotted. A mesh independence study was conducted and the least computationally expensive yet accurate mesh size was determined.

## 5.2 Scope for Future Work

SonicFoam solver solves for a pressure-velocity coupling. An extension of the current study can be undertaken in this direction, where a compressible density based solver such as rhoCentralFoam or rhoPimpleFoam is used for the same problem and the results obtained by both the solvers are compared. Another extension can be pursued by utilizing the LES Turbulence model for modeling the turbulence. Once again, the solutions obtained can be compared and the robustness of both the models for the given conditions can be determined.

A variation can be added to the study where the free stream mach number is also varied from a transonic regime to the limits of the supersonic regime. This would increase the application of the solutions to a wider range of problems involving supersonic airfoils.

While the above points deal with the inlet condition or solver settings, certain geometric variation can also be considered. For example, the thickness of the airfoil, blunt nose on the airfoil to reduce aerothermodynamic heating[3], other drag reducing modifications such as ducted airfoil [8], etc can also be incorporated.

# Bibliography


[1] John D Anderson Jr. *Hypersonic and high-temperature gas dynamics*. American Institute of Aeronautics and Astronautics, 2006.

[2] J.D. Anderson. *Modern Compressible Flow: With Historical Perspective*. McGraw-Hill series in aeronautical and aerospace engineering. McGraw-Hill, 1990. ISBN: 9780070016736. URL: https://books.google.co.in/books?id=P%5C_TDQgAACAAJ.

[3] James A Fay and Frederick R Riddell. "Theory of stagnation point heat transfer in dissociated air". In: *Journal of the Aerospace Sciences* 25.2 (1958), pp. 73–85.

[4] Weeratunge Malalasekera Henk Kaarle Versteeg. "An Introduction to Computational Fluid Dynamics: The Finite Volume Method". In: Washington, United States: Pearson Education Limited, 2007.

[5] Nelson H Kemp and FR Riddell. "Heat transfer to satellite vehicles re-entering the atmosphere". In: *Journal of Jet Propulsion* 27.2 (1957), pp. 132–137.

[6] Brian Edward Launder and Dudley Brian Spalding. "The numerical computation of turbulent flows". In: *Numerical prediction of flow, heat transfer, turbulence and combustion*. Elsevier, 1983, pp. 96–116.

[7] E. RATHAKRISHNAN. *GAS DYNAMICS*. PHI Learning, 2013. ISBN: 9788120348394. URL: https://books.google.co.in/books?id=uY31AAAAQBAJ.

[8] Stephen M Ruffin, Anurag Gupta, and David Marshall. "Supersonic channel airfoils for reduced drag". In: *AIAA journal* 38.3 (2000), pp. 480–486.

[9] Jorge Luis Garrido Tellez et al. "Evaluating Oblique Shock Waves Characteristics on a Double-Wedge Airfoil". In: *Engineering* 8.12 (2016), p. 862.

[10] *The OpenFOAM Foundation*. URL: https://openfoam.org/.